Nano World Journal

https://doi.org/10.17756/nwj.2023-s5-041

Review Article

Open Access

Utilization of Nanographene Oxide–Folic Acid–Metal Chalcogen in Cancer Theranostics

Souad A. Elfeky[1], Nayer Qenawi[1], Walid Tawfik[1*], Samah A. Loutfy[2] and T.D. Subash[3]

[1]*National Institute of Laser Enhanced Sciences, Cairo University, Cairo, Egypt*

[2]*Virology and Immunology Cancer Biology, Department of National Cancer Institute, Cairo University, Cairo, Egypt*

[3]*School of Information Engineering, Zhejiang Ocean University, Zhoushan, Zhejiang, China*

[*]Correspondence to:
Walid Tawfik
National Institute of Laser Enhanced Sciences,
Cairo University,
Cairo, Egypt.
E-mail: walid_tawfik@niles.edu.eg

Received: October 11, 2023
Accepted: December 18, 2023
Published: December 21, 2023

Citation: Elfeky SA, Qenawi N, Tawfik W, Loutfy SA, Subash TD. 2023. Utilization of Nanographene Oxide–Folic Acid–Metal Chalcogen in Cancer Theranostics. *NanoWorld J* 9(S5): S206-S214.

Published by United Scientific Group

Abstract

Background: In recent years, cancer theranostics (Diagnosis and treatment) has benefited greatly from using nanomedicine. Nanomaterials have unique biological properties that allow them to use in multi-therapeutic agents such as photo-thermal treatment (PTT) and photo-dynamic therapy (PDT) and diagnosis, so many researchers are trending recently to get a multimodal platform that achieves high efficiency in cancer theranostic.

Aim of review: This work discusses nanographene oxide (NGO) conjugated folic acid (FA), and some examples of NGO conjugated FA-nanohybrid and its applications in cancer theranostics and metal chalcogen and modified transition metal dichalcogenides (TMD) in cancer theranostics.

Key scientific concepts of review: The work underlines the chemistry, properties, and synthesis of NGO and how it can be conjugated with FA, then explains some examples of NGO-FA-nanohybrid and its application in cancer theranostics as NGO-FA-CuS, which represents NGO-FA-metal chalcogen which indicate that NGO-FA-metal chalcogen is a potential multimode theranostics agent for the advancement of cancer theranostics.

Keywords

Nanographene oxide, Folic acid, Metal chalcogen, Cancer, Theranostics.

Introduction

Cancer is a complex and multifaceted disease that can affect any part of the body and is characterized by the uncontrolled growth and spread of abnormal cells. Cancer remains one of the leading causes of death worldwide, despite advances in diagnosis and treatment choices brought about by cancer research. Cancer can have a serious impact on people and their families, underlining the need for continued efforts to prevent, identify, and cure this disease [1-3]. Cancer theranostics is a medical specialty combining therapeutic and diagnostic strategies to improve cancer treatment outcomes. The goal is to provide cancer patients with personalized therapy using targeted therapies based on specific tumour features. Cancer theranostics, which integrates diagnostic and therapeutic techniques, presents a viable option for more effective cancer treatment [3]. Because of the creation of novel nanoparticles (NPs) for diagnosing and treating diseases such as cancer, nanomedicine has undergone extraordinary growth in recent years [4, 5]. Because of their small size, NPs have unique biological features that allow them to have a higher surface area-to-volume ratio than other particles [6]. They can bind, absorb, and transport other molecules like proteins, probes, RNA (Ribonucleic acid), DNA (Deoxyribonucleic acid), and small-molecule drugs due to the size of their large functional surface area.

They are also highly stable, have a high carrier capacity, can incorporate both hydrophilic and hydrophobic substances, and are compatible with a variety of administration routes thanks to their tunable size, shape, and surface characteristics. This makes them highly appealing in many areas of medicine. Despite the fact that the design (i.e., shape and size) and substance from which NPs are created ultimately determines their physicochemical characteristics, nanoparticles are frequently stable throughout a wide temperature and pH range. Although certain NPs can't biodegrade and some dissolve slowly, this raises concerns regarding their safety, especially when used over an extended period of time. NPs are categorized as biologically inspired substances (phospholipids, lipids, dextran, and chitosan), carbon-based substances (carbon nanotubes), inorganic substances (those based on metals, for example, metals, metal oxides, and metal sulfides), as well as semiconductor substances (such as quantum dots (QDs)). Depending on their composition, how they interact with cells will vary [7]. The ideal theranostic NPs is one that is safe and biodegrades with non-toxic byproducts, selectively and swiftly accumulates in diseased tissue, reports local biochemical and morphological properties, and administers a non-invasive treatment [8]. Theranostic nanomaterials, despite serving the same objective, can gain from a number of factors that directly influence their physical-chemical, optoelectronic, and magnetic properties, as well as the success of the precise design of the intelligent nanodevice (Figure 1) [9].

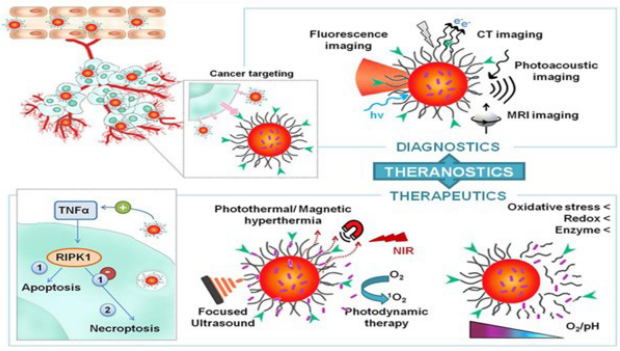

Figure 1: The term "theranostics" conceptually represented. To visualize, monitor, and treat the condition, theranostic NPs are created to be accumulated into the target region (tumor). For a multimodal clinical diagnosis and precise and individualized therapies, many therapeutic and diagnostic modalities can be integrated. Copyright Mauro et al. 2021 [9].

Graphene oxide (GO) and its derivatives, the most studied and employed delivery technology, have a variety of potential qualities that make them a promising candidate for cancer treatment. This NPs enhanced surface area, higher loading capacity, capacity to produce reactive oxygen species, and propensity for surface functionalization are some of its key properties. Numerous studies have revealed the remarkable efficacy of GO and its derivatives in cancer biosensing, gene delivery, medication delivery, photothermal therapy, combination therapy, concurrent therapy, and diagnostics (theranostics) [10]. The most significant flaw of cytotoxic anticancer drugs seen in figure 2 is their overall lack of selectivity, which frequently leads to systemic toxicity because of their inability to distinguish between cancerous and healthy cells. But rapidly proliferating cancer cells need a variety of vitamins and minerals, including folate.

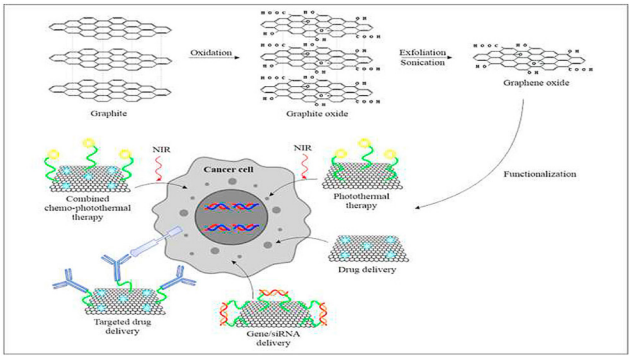

Figure 2: Various GO-based therapeutic strategies for the treatment of cancer. Copyright Alemi et al. 2020 [10].

As a result, cancer cells often overexpress folate uptake receptors. Folate receptors (FR), which FA binds to with a high affinity (0.1 - 1 nM), are thus particularly intriguing targets for selective drug-delivery and imaging-agents employing folate conjugates [11]. Notably, PTT and photoacoustic imaging have both been examined using 2D layered transition metal chalcogenide nanosheets, which demonstrate the benefits of synergistic diagnosis and treatment Thus six categories can be used to categorize the use of metal sulfide nanoparticles in cancer therapy: (1) MeSNs with outstanding structural and chemical properties can serve as anticancer drug carriers; (2) WS_2, MoS_2, and vanadium sulfide (VSx), which have strong light absorption coefficients, can be employed as phototherapeutic agents; (3) Radiotherapy can use high atomic number metal-containing MeSNs (such WS_2 and Bi_2S_3); (4) FeS and MnS are examples of MeSNs that can be employed as gas-generating agents. Additionally, the Fe^{2+} and Mn^{2+} that are produced from these MeSNs can function as Fenton catalysts for chemodynamic treatment; (6) Immunotherapy adjuvants can be made from MeSNs that can increase immunological responses in the body [12, 13].

In this review, utilization of GO conjugated FA – Metal chalcogen in cancer theranostics. First, we introduce GO synthesis and its properties and characterization. Then, conjugation of GO with FA. Then, the application of metal chalcogen in cancer theranostics. Last is experimental research of utilizing GO-FA-metal chalcogen in cancer theranostics.

GO NPs: Synthesis, Characterization, and Unique Properties

Since graphene is insoluble in water and is made up of thick layers of carbon atoms organized in hexagonal arrays and connected by sp2 hybridization, it can only be used as a passive platform for detection and cellular work. GO, its functional derivative, possesses distinctive qualities, mechanical and chemical stability, a 2D structure, and biocompatibility. Additionally, it offers a sizable, adaptable interface (which can be converted into a link) that enhances its effectiveness for biomedical applications and makes it simple to handle [14-16]. The hexagonal carbon structure of GO is similar to that of graphene, but it additionally includes oxygen-based functional groups such as alkoxy (C-O-C), hydroxyl (-OH),

carbonyl (C=O), carboxylic acid (-COOH), and others. These organizations Additionally, it is employed to create binding sites and change the surface characteristics of GO. It is appropriate for a variety of applications, including drug/gene delivery, phototherapy, and bioimaging, due to the presence of different molecules, including proteins, DNA, and RNA [17].

By oxidising powdered natural flake graphite, GO is easily produced. By combining a little amount of potassium chlorate with a graphite slurry in fuming nitric acid in 1859, the British chemist B.C. Brodie made the first effort to produce graphite oxide [9]. Staudenmaier enhanced this method in 1898 by utilizing a mixture of fuming nitric acid and strong sulfuric acid (H_2SO_4) and gradually adding chlorate to the reaction mixture. A straightforward and updated procedure for creating highly oxidized GO was made possible by this small tweak in the process [18]. Hoffmann's GO was created in 1937 using nitric acid and non-fuming potassium chlorate. Hummers published a different method for making graphene oxide in 1958 by combining potassium permanganate ($KMnO_4$) and sodium nitrate ($NaNO_3$) with concentrated sulfuric acid [19]. So, between 1859 and 1958, a number of techniques for producing GO were developed, including first the Brodie method then the Staudenmaier method after that the Hoffmann method, and finally the Hummers method, as well as their enhanced and modified variations (Figure 3) [20].

The most popular and efficient permanganate technique ever created was one by Hummers and Offeman. It is a traditional approach that can be used quickly for GO synthesis. Since then, other modified versions have been created, but their experimental methodology was largely the same as the original Hummers method, which used a $KMnO_4/H_2SO_4$ mixture for oxidation and hydrogen peroxide to stop the process [21]. In a nutshell, synthetic graphite powder (20 mm, with a purity of 99.99 wt.%) was used as the starting material to create GO utilizing the Hummers process. It explains how to make GO. Graphite (1 g), sodium nitrate (0.50 g), and concentrated H_2SO_4 (23 ml) were all put to a 500 ml flask that was held at 5 °C in an ice bath and stirred continuously for 5 min. The flask was then carefully filled with 3 g of $KMnO_4$ to avoid a significant reaction at certain locations. The reaction mixture was kept at 5 °C for 2 h, after which the temperature was gradually increased to 35 °C and maintained for an additional 30 min while being vigorously stirred. When 46 ml of deionized water was added to the suspension, the temperature rose to 98 °C as a result of hydration heat. With stirring, the bath was maintained at this temperature for 30 min. Deionized water (140 ml) and hydrogen peroxide (10% v/v, 10 ml) were added to stop the reaction. The solution was separated from the brownish-yellow end product using vacuum filtering. The remaining manganese ions and acid were then removed from the resulting GO powders by washing them five times in a 200 ml solution of diluted hydrochloric acid (5%) and warm (70 °C) deionized water, followed by a 12-h period of air drying at 60 °C. The concentration of $KMnO_4$ and $NaNO_3$ as well as the residence periods of the reaction mixture at the various phases were adjusted in order to create GO with various structures and O/C ratios [22].

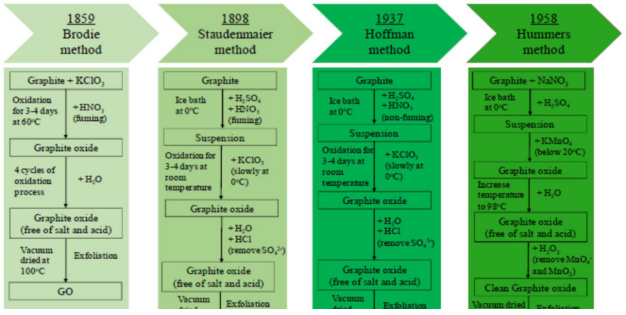

Figure 3: GO's general synthesis pathways. Copyright Hiew et al. 2018 [20].

Ultraviolet-Visible (UV-Vis), Fourier transform infrared (FTIR), and X-ray diffraction (XRD) spectroscopy were used to characterize the GO synthesized using various techniques. First, the GO's UV-Vis spectra were examined. Two distinct wavelengths showed absorption peaks. It is possible to detect GO using these two particular feature traits. The aromatic C-C bond π-π* transition is identified by the first peak for GO, which emerges at about 230 nm in wavelength. The second peak shoulder, which emerges at roughly 280 - 300 nm, is identified by the n-π* transition in the C=O bond [23, 24]. The FTIR approach revealed distinctive vibrational peaks for the different functional groups found in GO. For O-H stretching of hydroxyl groups, a broad peak was produced in the region of 3025 - 3435 cm^{-1}. High-intensity frequencies for the vibrational modes of the sp2 carbon structure and the carboxylic group's C=O were found at 1720 cm^{-1} and 1628 cm^{-1}, respectively. At 1409 cm^{-1}, 1225 cm^{-1}, and 1048 cm^{-1}, respectively, additional peaks representing C-O lengths of carboxyl, epoxy, and alkoxy functional groups were seen [24, 25].

The graphite was completely oxidized into GO, according to the XRD patterns of the 2θ peak, which can be observed at 9.03°. Furthermore, a d-spacing of 0.9794 nm (FWHM = 0.6298) was added to the GO interlayer distance. This increase has been caused by the intercalation of oxide functional groups such epoxy, hydroxyl, carbonyl, and carboxyl groups at the carbon basal plane during chemical oxidation reactions. As a result, there was an increase in the spacing between subsequent carbon layers [25]. Graphene is a flexible layered structure that is oxidized to form GO, which is embellished with hydroxyl, epoxy, and carboxyl groups on the edge and basal planes. GO is hydrophilic and readily disperses in a variety of liquids, including water, whereas graphene is hydrophobic and prone to aggregation.

Due to these characteristics, GO is simple to process and has a strong affinity for biomolecules. A deeper comprehension of the characteristics of graphene and its derivatives in the context of biology is necessary to expand the bio-applications of these materials. In vitro and in vivo, the majority of graphene and its derivatives are cyto-compatible [26]. The number of interactions that can take place on the surface of GO is increased by the presence of both aromatic (sp2) and aliphatic (sp3) domains [27]. For highly effective drug loading, single-layered GO has an ultra-high surface area accessible. The binding of different aromatic medicinal compounds is made possible by the delocalized p-electrons on the graphene plane through p-p stacking. Selective drug delivery to particular cancer cell types

can also be achieved by conjugating functionalized GO with targeted ligands [3, 28]. GO can become biocompatible after optimizing its structure and composition, making it highly promising for further clinical translation. The vast majority of research has shown that GO adequate surface engineering and key structural parameter controlling could significantly reduce the toxicity to cells *in vitro* or animals *in vivo* [29]. Figure 4 and figure 5 provide a schematic overview of how the inherent characteristics of GO affect its *in vitro* biocompatibility as well as a summary of the *in vivo* (preclinical) studies of GO, providing some guidance for the development of secure GO-based nanocarriers [30].

For prospective biotechnological applications, GO achieves outstanding aqueous processability, amphiphilicity, fluorescence quenching ability, surface functionalization capability, etc. In addition, a variety of biotechnological applications, including phototherapy, medication and gene delivery, bio-imaging, biosensing, and antibacterial action, have been made possible by nanocomposites of GO with gold and polymers as well as other magnetic nanoparticles [31].

FA: Properties, Advantages, and Conjugation of FA with GO and Applications in Cancer Theranostics

Vitamin B9/FA is crucial for the development of mammalian cells. It has also received substantial research as a targeted ligand for imaging and a number of cancer therapies. The FR (FA receptors), which are only found in small quantities in normal tissues but are increased on the surface of many cancer cells, have a high affinity for FA [32]. Because it is more stable and bioavailable than folate, FA, the fully oxidised mono glutamyl form of folate, is frequently utilized as a decorative ligand. Increased affinity and specificity for their receptors, superior conjugation qualities, low cost, easy availability, and non-immunogenicity are the benefits of FAs over other ligands. The FR are highly expressed in healthy tissues but have been found to be highly expressed in a number of malignancies, including nasopharyngeal, head and neck, breast, ovarian, endometrial, renal, and lung cancers [33].

In order to deliver nano-drugs that target ovarian cancer, folic acid and its analogues can bind specifically to folate receptors, enabling folate-modified NPs to penetrate tumour cells by receptor-mediated endocytosis [34]. A covalent amide bond was used to couple folic acid, a common target chemical for cancer cells, to NGO [35]. In order to boost NGO's stability in cell culture conditions containing 10% bovine serum, hydrophilic functional groups were added. First, the NGO sheet's OH groups have been changed to COOH groups. Then, using aryldiazonium salts of sulfanilic acid, SO_3H groups were added to the NGO sheets by sulfonation. The reaction between the NH_2 group of the FA molecule and the COOH group of the NGO-SO_3H led to the conjugation of FA with her NGO-SO_3H [36]. In a nutshell, GO (100 mg) synthesized using the modified Hummers and Offerman process was dissolved in 50 ml of deionized water before 2 g of sodium hydroxide and 2 g of sodium chloroacetate were added. After 30 min of sonication, the resultant mixture was

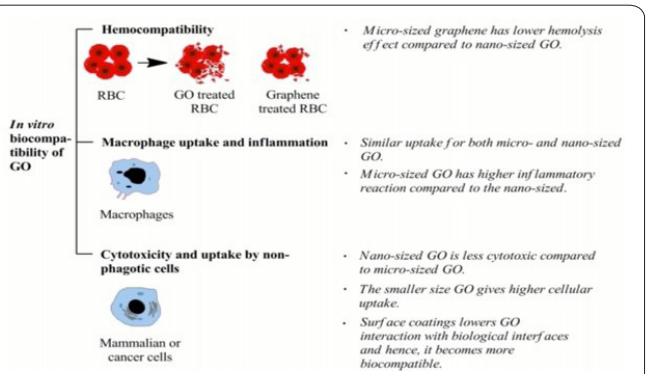

Figure 4: GO's *in vitro* biocompatibility includes its cytotoxicity, immunological response, macrophage uptake, and hemocompatibility. Copyright Kiew et al. 2016 [30].

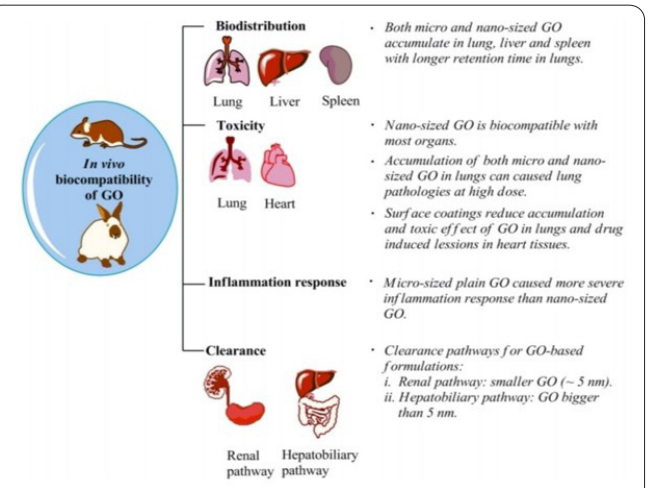

Figure 5: *In vivo* biocompatibility of GO: Bio-distribution, toxicity, inflammation response, and clearance. Copyright Kiew et al. 2016 [30].

neutralized with diluted hydrochloric acid. The resultant GO-COOH was then centrifuged apart and cleaned with deionized water. The diazonium salt solution (sulfanilic acid (200 mg) and $NaNO_3$ (75 mg) diluted in 50 ml of 0.25% sodium hydroxide solution and slowly added to 50 ml of 0.1 N hydrochloric acid) was then added to the GO-COOH after it had been dissolved in water. 50 ml of sodium hydroxide solution is gradually added. The resultant mixture was centrifuged and cleaned with deionized water after being agitated in an ice bath for two hours. GO-SO_3H (50 mg) was formed after 2 h of stirring in an ice bath, and then NHS (460 mg) and 1-ethyl-3-(3-dimethylaminopropyl) carbodiimide were added. (0.4 ml). It was then brought to a pH of 8 and stirred at room temperature for an hour before being combined with an FA solution (125 mg) dissolved in sodium bicarbonate. To create FA-bound GO (GO-FA), this mixture was mixed at room temperature for 4 h. It was gathered and cleaned using centrifugation and deionized water washing [37].

Excitation wavelength dependence was experimentally shown to provide a novel modality switch between therapy and imaging for the local targeting of cancer cells by FA-GO dual-functional agents [38]. According to Hamdy et al. FA-NGO-PVP was the ideal pH-responsive nanocarrier for the delivery of the anticancer medication doxorubicin (DOX) at loading levels greater than 100%. Next, near infrared (NIR)

PTT and chemotherapy were combined in *in vitro* trials. The outcomes demonstrated good efficacy for the treatment of cancer, since tailored chemo PTT could deliver medications and heat to the tumor site in a targeted manner. FA-NGO-PVP may therefore be a new nanomaterial for targeted chemo-PTT [39]. A new drug delivery system based on FA-conjugated-GO with superior solubility and minimal cytotoxicity can be created to target PDT, according to Huang et al. Through hydrophobic interactions and π–π stacking, PS (photosensitizer) Ce6 was successfully loaded into the system. Nanocarriers may considerably increase the formation of PS in cancer cells and have strong photodynamic effects on MGC803 cells [35].

The production and biological uses of FA-conjugated GO nanosheets functionalized with manganese dioxide (MnO_2) NPs were presented by Lim et al. When exposed to near-infrared light, FA-GO nanosheets can be employed for targeted PTT, whereas MnO_2 NPs can cause hypoxia by reducing hydrogen peroxide in the cancer microenvironment. NPs can also be employed as contrast materials in MRI imaging. MnO_2-FA-GO nanosheets were demonstrated. HeLa cells took it up, overexpressed the FA receptor, and were exposed to NIR radiation to cause hyperthermia (35% viability). For PTT and cancer-targeting applications, this composite MnO_2-FA-GO nanosheet may therefore be an effective carrier [36]. Cell uptake experiments by Hu et al. revealed that combining ZnO with GO-FA significantly improved cancer targeting. Due to the high electrical conductivity of graphene, the connection between graphene and ZnO, and the prevention of aggregation, GO-FA and ZnO hybrids considerably boost the photodynamic activity. They found that the photodynamic activity of noncytotoxic GO-FA-ZnO is mediated by the formation of reactive oxygen species (ROS) under visible light irradiation. Following the creation of ROS, GO-FA-ZnO led to notable reductions in cell viability, mitochondrial membrane potential, superoxide dismutase activity, catalase, and glutathione peroxidase, as well as an increase in the production of malondialdehyde. Furthermore, through raising caspase-3 activity, GO-FA-ZnO caused apoptotic death [40].

Metal Chalcogens in Cancer Theranostics

For the treatment of tumors, a number of types of materials have demonstrated efficacy as PTT agents. These include transition metal chalcogenides (CuS, Bi_2S_3, WO_{3-X}, and CuSe) and carbon nanomaterials (GO). Due to their narrow bandgaps and potent absorption properties, nanoscale metal sulfides, such as Ag_2S, Bi_2S_3, CdS, PbS, CuS, WS_2, and MoS_2 NPs, have received particular attention as theranostic nanoplatforms. For optical imaging, for instance, substantial research has been done on Ag_2S, PbS, and CdS, and the biolabeling of Bi_2S_3 and CuS NPs has proven to be a superb multimodal theranostic platform for cancer therapy [24]. Due to their advantages such as tunable/flexible optical behavior, biocompatibility, lack of toxicity, renal clearance, facile chemical, and biological manufacturing, etc. Metal sulfide NPs. It is a crucial tool for the prevention, detection, and treatment of cancer. Due to their cytotoxicity, zinc and copper sulfides are also utilized in theranostics. Using gamma-ray detectors, rhenium sulfide has been investigated for mapping the sentinel lymph node of different malignancies, including the breast, oesophagus, and stomach [41].

2D TMD nanomaterials are intriguing for biological applications like bioimaging, drug administration, and improved PTT and RT (Radiotherapy) because they have characteristics like strong NIR absorption, adjustable components, and good X-ray attenuation capabilities. A nanoplatform, that is. With regard to developing highly effective and accurate cancer treatments, 2D TMD in particular offers enormous potential as a platform for merging RT and PTT with other therapeutic and imaging capacities [42]. 2D transition metal sulfides commonly exhibit unusual electrical and visual properties as a result of quantum confinement. When the bulk counterpart is reduced to a single monolayer substance, the surface effects of the indirect to direct bandgap transition are observed. Moreover, this tunable bandgap characteristic frequently coexists with strong photoluminescence and high exciton binding energies. As a result, numerous conventional metal complexes, including MoS_2, SnS, and TaS_2, have been discovered in biomedicine, particularly PTT, and biosensing [43].

Metal transition-sulfides (MTSs), which have the general formula MS_{2x} and display distinctive physical and chemical properties, are among the most well-studied nanostructured metal chalcogenides in PDT. They can crystallize into one of the following three primary types of structures, depending on the metal content: pyrite (FeS_2), molybdenite type (MoS_2), or CdI_2-type. MTS nanostructures with distinctive physicochemical properties used in theranostics are caused by this heterogeneity in composition and structure. Their high NIR absorption in the 700 - 1100 nm range, which can be used for phototherapy, medication delivery, and bioimaging probes, offers enormous potential benefits for theranostic applications. There has been a lot of research done on MTSs' characteristics, such as their high extinction coefficients, adaptive surface chemistry, strong fluorescence, magnetism, structural stability, and thermal stability. Moreover, MTSs are easier to make using low-cost synthetic methods than other NIR-absorbing metal NPs including gold, silver, and copper [44].

Modified TMDs in Cancer Theranostics

Liu et al. created nanocomposites of MoS_2/GO. It demonstrated acceptable biocompatibility *in vitro* and *in vivo* as well as good dispersibility in aqueous solutions. MoS_2/GO demonstrated a novel capacity to target the lung specifically, which is significant. In other words, when aimed at the lung, MoS_2/GO had a distinct propensity to localize there similar to GO, producing a "guided missile" effect. Additionally, the MoS_2/GO composites had a better ability to load drugs and had a stronger tumoricidal effect on cancer cells that frequently metastasis to the lung. Importantly, MoS_2/GO composites effectively slowed the formation of metastatic tumors caused by B16 murine melanoma cancer cells in mice lungs [45].

Based on the difference in precursor solubility in various solvents, Zhao et al. offer for the first time an easy and distinctive outside-in method to synthesize high dispersive mesoporous silica nanoparticle (MSN)/MoS_2-PEG NPs (SMPs). The generated SMPs, which could be employed for the combination of tumor-hyperthermia and chemotherapy, exhibit a high drug loading efficiency of 64.7% owing to the mesoporous silica pore structure and a good photothermal performance of 41.5% thanks to the internally decorated MoS_2 nanosheets. Results from *in vivo* experiments indicate that SMPs have a considerable synergistic effect; specifically, the heat produced during PTT can boost DOX's sensitivity to chemotherapy and hence synergistically improve its therapeutic effect. Such an easy procedure gives a new uncomplicated method to generate a novel theranostic agent by combining many functionalities into a single dosage and demonstrates a viable method to create nanomaterials utilizing MSN as a template [46].

In order to attain improved characteristics, Chacko et al. effectively created a distinctive 2D-MoS_2-based nanocomposite by adding ZnO (zinc oxide) NPs using a straightforward hydrothermal process. The creation of pure hexagonal MoS_2 and ZnO structures as well as the blending of ZnO and MoS_2 to create a nanocomposite are both confirmed by structural analyses. The direct electronic transitions in the Brillouin zone's K-point are demonstrated through optical studies. It's interesting to note that the nanostructures displayed down- and up-conversion photo-luminescence phenomena that were excitation wavelength dependent. The MoS_2-ZnO nanocomposite's coupling was made stronger by the development of a wasp-waisted hysteresis loop. Studies on the bioactivity of these particles showed that they have a Biosafety Index of almost 2 and selective cytotoxic action against cancer cells. The nanocomposite modulates all three stages of cancer formation, including (a) cellular proliferation by inducing apoptosis, (b) tumor vascularization by reducing angiogenesis, and (c) metastatic potential by suppressing epithelial-mesenchymal transition, according to mechanistic analyses. Therefore, these investigations aid in the development of MoS_2-based nanocomposites for cutting-edge cancer theranostics applications [47].

According to Gao et al. a straightforward solvothermal process was used to create rod-shaped Bi_2S_3-MoS_2 heterogeneous nanoparticles (BMNPs). With a high X-ray attenuation coefficient and acceptable heating-inductive capabilities when exposed to NIR radiation, the latter performs as an effective dual-role nano-re-radiosensitizer. The quasi-threshold X-ray dose can be decreased from 1.39 Gy to 0.92 Gy as a result, and the sensitivity ratio can be improved by 17.9% (from 0.95 to 1.12). The increased radiosensitization brought on by BMNP may be due to increased tumour oxygenation and DNA damage brought on by ROS, which may limit the ability of cancer cells to self-heal. Additionally, by administering the produced BMNPs to tumor-bearing mice, computed tomography and photoacoustic (CT-PA) imaging can be used to pinpoint the tumor's location. These characteristics distinguish BMNPs as dual-mode radiosensitizers for synergetic theranostic imaging of triple-negative breast cancer in addition to preventing metastasis [48].

Using physical grinding and ultrasonication, Yong et al. described a straightforward, environmentally friendly procedure for creating a multifunctional nanomedicine based on WS_2 QDs. The resulting small-sized (3 nm) WS_2 QDs have obvious PTT/RT synergistic effects for the treatment of tumours in addition to powerful X-ray CT-PA signal enhancement. After intravenous injection of WS_2 QDs, the tumour is precisely positioned and completely destroyed *in vivo* thanks to CT/PA imaging and the synergistic action between PTT and RT [33]. According to Wang et al.'s research, WS_2-PEG NPs have a good chance of being effective clinical CT-guided photothermal anticancer treatments [49].

For the one-pot hydrothermal and controlled synthesis of surface-modified WS_2 nanosheets incorporating polyvinylpyrrolidone (PVP), Wang et al. presented a bottom-up approach. The material was created using the chelate-coordination effect between the oxygen lone electron pair of the PVP carbonyl group and the vacant orbital (5d orbital) of tungsten. Excellent photothermal conversion performance was shown by WS_2 nanosheets with synchronous surface-PVP grafting, and the surface-anchored PVP ensured colloidal stability. Additionally, the excellent X-ray attenuation capabilities and NIR absorption of WS_2-PVP_{360kDa} enabled sensitive *in vitro* and *in vivo* CT/PA imaging. Additionally, the excellent X-ray attenuation capabilities and NIR absorption of WS_2-PVP_{360kDa} enabled sensitive *in vitro* and *in vivo* CT/PA imaging. The WS_2-PVP_{360kDa} nanosheets showed promising *in vitro* and *in vivo* antitumor effectiveness and were biocompatible [50].

When applied to human bronchial cells (BEAS-2B), WS_2 and MoS_2 NPs cause cytotoxicity and pro-inflammatory reactions [51]. A brand-new molybdenum selenide nanosheet-based nanohybrid for PA imaging and PTT is presented by Chen et al. as s$MoSe_2$-ICG-NSs. A single layer of s$MoSe_2$-NSs molybdenum selenide nanosheets and ICG are covalently coupled. After confirming its effects on PAI and PTT *in vitro*, the s$MoSe_2$-ICG NS agent is used for extremely sensitive, highly effective tumour PTT *in vivo* [52]. Jia et al. describe the creation and application of a novel therapeutic platform based on PS-loaded 2D layered nanomaterials called WSe_2 for the treatment of cancer using both PTT and PDT methods. The WSe_2-BSA nanosheets are efficient photothermal agents, methylene blue (MB) carriers, and PS agents for PDT. Additionally, modulating singlet oxygen generation using NIR irradiation can control the release of MB from the WSe_2 nanosheets. Both *in vitro* and *in vivo* research was done on the therapeutic effectiveness of WSe_2-BSA (WSe_2-BSA/MB) conjugates on cancer cells. Dual-mode PTT-PDT therapy was found to considerably improve therapeutic efficacy when compared to single-mode therapy. These findings suggest that WSe_2 nanosheets have potential as therapeutic agents and could act as an intelligent carrier for complementing applications in phototherapy and biomedicine [53].

Experimental Research on the Usage of NGO-FA-Metal Chalcogen in Cancer Theranostic

To advance photothermal therapy for cancer, Gururaj et al. present a logical synthesis of NGO-FA-CuS, a multimodal photothermal agent. FA was covalently conjugated to NGO via an amide bond, and a hierarchical structure of NGO-FA-CuS was produced as a result [37]. The FAs were covalently linked to the NGOs in this method rather than being mixed or deposited, which helped to preserve their intrinsic properties following conjugation and made them accessible in the resulting hybrid nanostructures. The NGO-FA-CuS photothermal agent was specifically created with each component playing a specific purpose. Quenchers, cancer cell-targeting molecules, and photothermal conversion agents, respectively, are the roles played by NGO, FA, and CuS. Prior to the implantation of FA molecules and the deposition of CuS nanoflowers, sulfonic acid groups were added to NGOs to guarantee their stability under physiological conditions. NGO-FA-CuS can heat up to 63.1 °C in just 5 min after being exposed to a 980 nm laser, which is much higher than the temperature at which cancer cells can survive. As a result, the NGO-FA-CuS temperatures were high enough to kill cancer cells by inducing hyperthermia in them. NGO-FA-CuS rapidly warms their nuclei when exposed to a NIR laser, eradicating their genetic material, and inducing radical apoptosis. NGO-FA-CuS showed outstanding photothermal efficiency of 46.2% and excellent cytotoxicity against HeLa, SKOV3, and KB cells when exposed to a 980 nm laser. Additionally, NGO-FA-CuS demonstrates outstanding persistent photostability and is non-photo corrosive. The amount of NGO-FA-CuS present and the laser's power density also have an impact on the photothermal effect. Finally, it was discovered that increasing NGO-FA-CuS concentration and incubation duration increased the cytotoxicity of the compound against cancer cells [37].

Conclusion

The work described in this article investigates NGO chemistry, properties, and synthesis conjugated with FA. The details are given about some examples of NGO-FA-nanohybrid and its application in cancer theranostics as NGO-FA-CuS. The latter represents NGO-FA-metal chalcogen as a potential multimode theranostics agent for advancing cancer theranostics. Further applications were given in using the NGO-FA-metal chalcogen in multi-therapeutic agents, such as PTT and PDT therapies and diagnosis. The properties of NGO-FA-metal chalcogen allow one to prepare a multimodal to improve the efficiency of cancer treatment approaches and diagnosis techniques in future applications.

Acknowledgements

This paper is based upon work supported by Science, Technology & Innovation Funding Authority (STDF) under grant number 45893.

Conflict of Interest

None.

References

1. Zubair H, Ahmad A. 2017. Cancer Metastasis: An Introduction. In Ahmad A (ed) Introduction to Cancer Metastasis. Academic Press, pp 3-12.
2. Saini A, Kumar M, Bhatt S, Saini V, Malik A. 2020. Cancer causes and treatments. *Int J Pharm Sci Res* 11(7): 3121-3134. https://doi.org/10.13040/IJPSR.0975-8232.11(7).3109-22
3. Gamal H, Tawfik W, El-Sayyad HH, Fahmy HM, Emam AN, et al. 2023. Efficacy of polyvinylpyrrolidone-capped gold nanorods against 7,12 dimethylbenz(a)anthracene-induced oviduct and endometrial cancers in albino rats. *Egypt J Basic Appl Sci* 10(1): 274-289. https://doi.org/10.1080/2314808X.2023.2185615
4. Ahmed N, Liaqat U, Rafique M, Baig MA, Tawfik W. 2020. Detection of toxicity in some oral antidiabetic drugs using LIBS and LA-TOF-MS. *Microchem J* 155: 104679. https://doi.org/10.1016/j.microc.2020.104679
5. Alqahtani SF, Farooq WA, Ali SM, Tawfik W. 2019. Fabrication and study of structural and optical properties of cadmium telluride quantum dots. *J Optoelectron Adv Mater* 21: 385-394.
6. Ezzat H, Menazea AA, Omara W, Basyouni OH, Helmy SA, et al. 2020. DFT: B3LYP/LANL2DZ study for the removal of Fe, Ni, Cu, As, Cd and Pb with Chitosan. *Biointerface Res Appl Chem* 10: 7002-7010. https://doi.org/10.33263/BRIAC106.70027010
7. Thakor AS, Gambhir SS. 2013. Nanooncology: the future of cancer diagnosis and therapy. *CA Cancer J Clin* 63(6): 395-418. https://doi.org/10.3322/caac.21199
8. Jokerst JV, Gambhir SS. 2011. Molecular imaging with theranostic nanoparticles. *Acc Chem Res* 44(10): 1050-1060. https://doi.org/10.1021/ar200106e
9. Mauro N, Utzeri MA, Varvarà P, Cavallaro G. 2021. Functionalization of metal and carbon nanoparticles with potential in cancer theranostics. *Molecules* 26(11): 3085. https://doi.org/10.3390/molecules26113085
10. Alemi F, Zarezadeh R, Sadigh AR, Hamishehkar H, Rahimi M, et al. 2020. Graphene oxide and reduced graphene oxide: efficient cargo platforms for cancer theranostics. *J Drug Deliv Sci Technol* 60: 101974. https://doi.org/10.1016/j.jddst.2020.101974
11. Geersing A, de Vries RH, Jansen G, Rots MG, Roelfes G. 2019. Folic acid conjugates of a bleomycin mimic for selective targeting of folate receptor positive cancer cells. *Bioorg Med Chem Lett* 29(15): 1922-1927. https://doi.org/10.1016/j.bmcl.2019.05.047
12. Wu J, Zhang S, Mei X, Liu N, Hu T, et al. 2020. Ultrathin transition metal chalcogenide nanosheets synthesized via topotactic transformation for effective cancer theranostics. *ACS Appl Mater Interfaces* 12(43): 48310-48320. https://doi.org/10.1021/acsami.0c13364
13. Fei W, Zhang M, Fan X, Ye Y, Zhao M, et al. 2021. Engineering of bioactive metal sulfide nanomaterials for cancer therapy. *J Nanobiotechnol* 19(1): 1-27. https://doi.org/10.1186/s12951-021-00839-y
14. Priyadarsini S, Mohanty S, Mukherjee S, Basu S, Mishra M. 2018. Graphene and graphene oxide as nanomaterials for medicine and biology application. *J Nanostruct Chem* 8: 123-137. https://doi.org/10.1007/s40097-018-0265-6
15. Rhazouani A, Gamrani H, El Achaby M, Aziz K, Gebrati L, et al. 2021. Synthesis and toxicity of graphene oxide nanoparticles: a literature review of *in vitro* and *in vivo* studies. *Biomed Res Int* 2021: 5518999. https://doi.org/10.1155/2021/5518999
16. Liu L, Ma Q, Cao J, Gao Y, Han S, et al. 2021. Recent progress of graphene oxide-based multifunctional nanomaterials for cancer treatment. *Cancer Nanotechnol* 12: 1-31. https://doi.org/10.1186/s12645-021-00087-7

17. Menazea AA, Ezzat HA, Omara W, Basyouni OH, Ibrahim SA, et al. 2020. Chitosan/graphene oxide composite as an effective removal of Ni, Cu, As, Cd and Pb from wastewater. *Comput Theor Chem* 1189: 112980. https://doi.org/10.1016/j.comptc.2020.112980
18. Staudenmaier L. 1898. Verfahren zur darstellung der graphitsäure. *Berichte Deutsch Chem Gesellschaft* 31(2): 1481-1487. https://doi.org/10.1002/cber.18980310237
19. Hummers Jr WS, Offeman RE. 1958. Preparation of graphitic oxide. *J Am Chem Soc* 80(6): 1339-1339. https://doi.org/10.1021/ja01539a017
20. Hiew BYZ, Lee LY, Lee XJ, Thangalazhy-Gopakumar S, Gan S, et al. 2018. Review on synthesis of 3D graphene-based configurations and their adsorption performance for hazardous water pollutants. *Process Saf Environ Prot* 116: 262-286. https://doi.org/10.1016/j.psep.2018.02.010
21. Yoo MJ, Park HB. 2019. Effect of hydrogen peroxide on properties of graphene oxide in Hummers method. *Carbon* 141: 515-522. https://doi.org/10.1016/j.carbon.2018.10.009
22. Guerrero-Contreras J, Caballero-Briones F. 2015. Graphene oxide powders with different oxidation degree, prepared by synthesis variations of the Hummers method. *Mater Chem Phys* 153: 209-220. https://doi.org/10.1016/j.matchemphys.2015.01.005
23. Kigozi M, Koech RK, Kingsley O, Ojeaga I, Tebandeke E, et al. 2020. Synthesis and characterization of graphene oxide from locally mined graphite flakes and its supercapacitor applications. *Results Mater* 7: 100113. https://doi.org/10.1016/j.rinma.2020.100113
24. Chaudhary M, Seugar RS, Yadav MK, Kumar M, Kumar P. 2019. Synthesis and characterization of graphene oxide. *Prog Agric* 19(1): 158-160. https://doi.org/10.5958/0976-4615.2019.00028.0
25. Hidayah NMS, Liu WW, Lai CW, Noriman NZ, Khe CS, et al. 2017. Comparison on graphite, graphene oxide and reduced graphene oxide: synthesis and characterization. *AIP Conf Proc* 1892: 150002. https://doi.org/10.1063/1.5005764
26. Li J, Liu X, Crook JM, Wallace GG. 2019. 3D graphene-containing structures for tissue engineering. *Mater Today Chem* 14: 100199. https://doi.org/10.1016/j.mtchem.2019.100199
27. Yu W, Sisi L, Haiyan Y, Jie L. 2020. Progress in the functional modification of graphene/graphene oxide: a review. *RSC Adv* 10(26): 15328-15345. https://doi.org/10.1039/d0ra01068e
28. Yang K, Feng L, Shi X, Liu Z. 2013. Nano-graphene in biomedicine: theranostic applications. *Chem Soc Rev* 42(2): 530-547. https://doi.org/10.1039/c2cs35342c
29. Zhou Y, Jing X, Chen Y. 2017. Material chemistry of graphene oxide-based nanocomposites for theranostic nanomedicine. *J Mater Chem B* 5(32): 6451-6470. https://doi.org/10.1039/c7tb00680b
30. Kiew SF, Kiew LV, Lee HB, Imae T, Chung LY. 2016. Assessing biocompatibility of graphene oxide-based nanocarriers: a review. *J Control Release* 226: 217-228. https://doi.org/10.1016/j.jconrel.2016.02.015
31. Banerjee AN. 2018. Graphene and its derivatives as biomedical materials: future prospects and challenges. *Interface Focus* 8(3): 20170056. https://doi.org/10.1098/rsfs.2017.0056
32. Ngernyuang N, Seubwai W, Daduang S, Boonsiri P, Limpaiboon T, et al. 2016. Targeted delivery of 5-fluorouracil to cholangiocarcinoma cells using folic acid as a targeting agent. *Mater Sci Eng C* 60: 411-415. https://doi.org/10.1016/j.msec.2015.11.062
33. Yugui F, Wang H, Sun D, Zhang X. 2019. Nasopharyngeal cancer combination chemoradiation therapy based on folic acid modified, gefitinib and yttrium 90 co-loaded, core-shell structured lipid-polymer hybrid nanoparticles. *Biomed Pharmacother* 114: 108820. https://doi.org/10.1016/j.biopha.2019.108820
34. Chuan D, Mu M, Hou H, Zhao N, Li J, et al. 2021. Folic acid-functionalized tea polyphenol as a tumor-targeting nano-drug delivery system. *Mater Des* 206: 109805. https://doi.org/10.1016/j.matdes.2021.109805
35. Huang P, Xu C, Lin J, Wang C, Wang X, et al. 2011. Folic acid-conjugated graphene oxide loaded with photosensitizers for targeting photodynamic therapy. *Theranostics* 1: 240-250. https://doi.org/10.7150/thno/v01p0240
36. Lim JH, Kim DE, Kim EJ, Ahrberg CD, Chung BG. 2018. Functional graphene oxide-based nanosheets for photothermal therapy. *Macromol Res* 26(6): 557-565. https://doi.org/10.1007/s13233-018-6067-3
37. Neelgund GM, Oki A. 2021. Folic acid and CuS conjugated graphene oxide: an efficient photocatalyst for explicit degradation of toxic dyes. *Appl Surf Sci* 566: 150648. https://doi.org/10.1016/j.apsusc.2021.150648
38. Jun SW, Kwon J, Chun SK, Lee HA, Lee J, et al. 2018. Modality switching between therapy and imaging based on the excitation wavelength dependence of dual-function agents in folic acid-conjugated graphene oxides. *Biomed Opt Express* 9(2): 705-716. https://doi.org/10.1364/BOE.9.000705
39. Hamdy O, Tawfik W. 2020. The effect of temperature on the optical and analytical properties of PET polymer used in drinking water bottles. *J Phys Conf Ser* 1472: 012004. https://doi.org/10.1088/1742-6596/1472/1/012004
40. Hu Z, Li J, Li C, Zhao S, Li N, et al. 2013. Folic acid-conjugated graphene–ZnO nanohybrid for targeting photodynamic therapy under visible light irradiation. *J Mater Chem B* 1(38): 5003-5013. https://doi.org/10.1039/c3tb20849d
41. Farooq WA, Tawfik W, Fatehmulla A, Ali SM, Aslam M. 2013. Laser irradiation effect on ZnO nanoparticles. In International Conference on Advanced Optoelectronics and Lasers, Sudak, Ukraine.
42. Cheng L, Wang X, Gong F, Liu T, Liu Z. 2020. 2D nanomaterials for cancer theranostic applications. *Adv Mater* 32(13): 1902333. https://doi.org/10.1002/adma.201902333
43. Qin XC, Guo ZY, Liu ZM, Zhang W, Wan MM, et al. 2013. Folic acid-conjugated graphene oxide for cancer targeted chemo-photothermal therapy. *J Photochem Photobiol B Biol* 120: 156-162. https://doi.org/10.1016/j.jphotobiol.2012.12.005
44. Diaz-Diestra D, Gholipour HM, Bazian M, Thapa B, Beltran-Huarac J. 2022. Photodynamic therapeutic effect of nanostructured metal sulfide photosensitizers on cancer treatment. *Nanoscale Res Lett* 17(1): 33. https://doi.org/10.1186/s11671-022-03674-8
45. Liu Y, Peng J, Wang S, Xu M, Gao M, et al. 2018. Molybdenum disulfide/graphene oxide nanocomposites show favorable lung targeting and enhanced drug loading/tumor-killing efficacy with improved biocompatibility. *NPG Asia Mater* 10(1): e458-e458. https://doi.org/10.1038/am.2017.225
46. Zhao J, Xie P, Ye C, Wu C, Han W, et al. 2018. Outside-in synthesis of mesoporous silica/molybdenum disulfide nanoparticles for antitumor application. *Chem Eng J* 351: 157-168. https://doi.org/10.1016/j.cej.2018.06.101
47. Chacko L, Poyyakkara A, Kumar VS, Aneesh PM. 2018. MoS_2-ZnO nanocomposites as highly functional agents for anti-angiogenic and anti-cancer theranostics. *J Mater Chem B* 6(19): 3048-3057. https://doi.org/10.1039/c8tb00142a
48. Gao F, Wang D, Zhang T, Ghosal A, Guo Z, et al. 2020. Facile synthesis of Bi_2S_3-MoS_2 heterogeneous nanoagent as dual functional radiosensitizer for triple negative breast cancer theranostics. *Chem Eng J* 395: 125032. https://doi.org/10.1016/j.cej.2020.125032
49. Wang JT, Zhang W, Wang WB, Wu YJ, Zhou L, et al. 2019. One-pot bottom-up fabrication of biocompatible PEGylated WS_2 nanoparticles for CT-guided photothermal therapy of tumors *in vivo*. *Biochem Biophys Res Commun* 511(3): 587-591. https://doi.org/10.1016/j.bbrc.2019.01.009
50. Gamal H, Tawfik W, El-Sayyad HH, Fahmy HM, Emam AN, et al. 2023. Efficacy of polyvinylpyrrolidone-capped gold nanorods against 7,12 dimethylbenz(a)anthracene-induced oviduct and endometrial cancers in albino rats. *Egypt J Basic Appl Sci* 10(1): 274-289. https://doi.org/10.1080/2314808X.2023.2185615

51. Zapór L, Chojnacka-Puchta L, Sawicka D, Miranowicz-Dzierżawska K, Skowroń J. 2022. Cytotoxic and pro-inflammatory effects of molybdenum and tungsten disulphide on human bronchial cells. *Nanotechnol Rev* 11(1): 1263-1272. https://doi.org/10.1515/ntrev-2022-0073

52. Gamal H, Tawfik W, Fahmy HM, El-Sayyad HH. 2021. Breakthroughs of using photodynamic therapy and gold nanoparticles in cancer treatment. In IEEE International Conference on Nanoelectronics, Nanophotonics, Nanomaterials, Nanobioscience & Nanotechnology (5NANO), Kottayam, Kerala, India.

53. Jia X, Bai J, Ma Z, Jiang X. 2017. BSA-exfoliated WSe_2 nanosheets as a photoregulated carrier for synergistic photodynamic/photothermal therapy. *J Mater Chem B* 5(2): 269-278. https://doi.org/10.1039/c6tb02525k